



Hypoxia Delays Oligodendrocyte Progenitor Cell Migration and Myelin Formation by Suppressing Bmp2b Signaling in Larval Zebrafish

Lei-qing Yang¹, Min Chen¹, Jun-long Zhang¹, Da-long Ren^{1*} and Bing Hu^{1,2*}

¹ Hefei National Laboratory for Physical Sciences at the Microscale, School of Life Sciences, University of Science and Technology of China, Hefei, China, ² Chinese Academy of Sciences Key Laboratory of Brain Function and Disease, School of Life Sciences, University of Science and Technology of China, Hefei, China

OPEN ACCESS

Edited by:

Stefania Ceruti,
Università degli Studi di Milano, Italy

Reviewed by:

Mario Valentino,
University of Malta, Malta
Anil Kumar Challa,
The University of Alabama
at Birmingham, United States

*Correspondence:

Da-long Ren
rendl8736@ustc.edu.cn
Bing Hu
bhu@ustc.edu.cn

Received: 29 June 2018

Accepted: 18 September 2018

Published: 04 October 2018

Citation:

Yang L-q, Chen M, Zhang J-l, Ren D-l and Hu B (2018) Hypoxia Delays Oligodendrocyte Progenitor Cell Migration and Myelin Formation by Suppressing Bmp2b Signaling in Larval Zebrafish. *Front. Cell. Neurosci.* 12:348. doi: 10.3389/fncel.2018.00348

Hypoxia in newborns tends to result in developmental deficiencies in the white matter of the brain. As previous studies of the effects of hypoxia on neuronal development in rodents and human infants have been unable to use *in vivo* imaging, insight into the dynamic development of oligodendrocytes (OLs) in the central nervous system under hypoxia is limited. Here, we developed a visual model to study OL development using sublethal postnatal hypoxia in zebrafish larvae. We observed that hypoxia significantly suppressed OL progenitor cell migration toward the dorsum using *in vivo* imaging. Further, we found that hypoxia affected myelination, as indicated by thinner myelin sheaths and by a downregulation of myelin basic protein expression. Bmp2b protein expression was also significantly downregulated following hypoxia onset. Using gain of function and loss of function experiments, we demonstrated that the Bmp2b protein was associated with the regulation of OL development. Thus, our work provides a visual hypoxia model within which to observe OL development *in vivo*, and reveals the underlying mechanisms involved in these processes.

Keywords: hypoxia, oligodendrocyte, differentiation, myelination, bmp2b, zebrafish

INTRODUCTION

Prior clinical research has indicated that adequate oxygen delivery is vital for brain development in infants (Hack et al., 2000; Back et al., 2006; Chahboune et al., 2009). Many investigators have modeled clinical symptoms in experimental animals by exposing neonatal rodents to different degrees and durations of hypoxia (Ganat et al., 2002; Kanaan et al., 2006; Zhou et al., 2008; Fagel et al., 2009). In both mice and rats, hypoxia reduces the volumes of the cerebral cortex and corpus callosum, and eventually leads to liberal ventriculomegaly (Weiss et al., 2004; Watzlawik et al., 2015). Hypoxia also has been shown to disrupt synaptic development (Curristin et al., 2002), binuclear neuron formation (Paltsyn et al., 2014), and glia–neuron interactions (Accorsi-Mendonca et al., 2015). Thus, hypoxia presumably abrogates the development and cognitive potential of the newborn brain (Huppi et al., 2001; Sabatino et al., 2003). A recent study demonstrated that targeting EGFR in oligodendrocyte (OL) progenitor cells (OPCs) at a specific time after premature newborn hypoxic injury was clinically feasible and potentially beneficial (Scafidi et al., 2014). Thus, it is clear that hypoxia plays an important role in the development of neurons and glia in the brain. However,

neural behavior, especially OL behavior, in the spinal cord has rarely been monitored *in vivo* in conjunction with hypoxia.

Zebrafish (*Danio rerio*) represent an attractive vertebrate model for developmental research due to their rapid development (Kimmel et al., 1995) and transparency, allowing easy *in vivo* imaging. Moreover, as mammalian and zebrafish OLs and myelin are homologous, the transparent zebrafish model represents an efficient tool for the observation of OL differentiation and myelination; using zebrafish, it is also possible to explore molecular mechanisms *in vivo* via a number of previously described genetic manipulations and fluorescence transgeneses (Buckley et al., 2008; Dubois-Dalcq et al., 2008; He et al., 2014). Although hypoxia-induced retinopathy (Cao et al., 2010), bone regeneration (Maes et al., 2012), and cancer metastasis (Kumar and Gabrilovich, 2014) have been widely studied, little is known about the mechanism of OL development in the hypoxic zebrafish model.

Here, we found that hypoxia inhibited OPC dorsal migration, delayed the onset of OL myelination *in vivo*, and reduced the expression of the *mbp* gene. Transmission electron microscope (TEM) images showed a thinner myelin sheath in response to hypoxic conditions. We used molecular methods to show that the *bmp2b* gene was downregulated under hypoxia. Using a Bmp2b receptor inhibitor and *bmp2b* messenger RNA (mRNA) rescue strategy, we demonstrated that Bmp2b participated in regulating OL development under hypoxia. Collectively, our findings indicated that hypoxia suppresses OL differentiation via Bmp2b signaling.

MATERIALS AND METHODS

Zebrafish Lines and Maintenance

The following zebrafish lines were used in this study: wild-type (WT), transgenic OL lineage transcription factor 2 labeled by EGFP [Tg (*olig2*:EGFP)] (Shin et al., 2003), Tg (*mbp*:EGFP-CAAX; donated by Prof. David A. Lyons, University of Edinburgh, Edinburgh, United Kingdom) (Almeida et al., 2011) and Tg (Tol-056) (Satou et al., 2009). Zebrafish embryos were bred with laboratory stock and were maintained at 28.5°C with a 14/10 h light/dark cycle. Zebrafish embryos were collected from natural spawning and staged by days post-fertilization (dpf), according to established criteria (Kimmel et al., 1995). To prevent dark pigment formation, larvae were raised in an embryo medium containing 0.2 mM *N*-phenylthiourea (Sigma-Aldrich, St. Louis, MO, United States).

All of the animal manipulations described in this study were conducted in strict accordance with the guidelines and regulations set forth by the University of Science and Technology of China (USTC) Animal Resources Center and University Animal Care and Use Committee. All protocols were approved by the Committee on the Ethics of Animal Experiments of the USTC (permit no. USTCACUC1103013).

Hypoxia Device

The hypoxia device we used contained a self-driven unit that automatically controlled nitrogen gas perfusion depending on

dissolved oxygen levels in the water (Cao et al., 2010). An oxygen electrode was connected to an oxygen regulator and to the nitrogen gas supplier to accurately detect oxygen levels continuously. We used 100% of the ambient oxygen in the air (7.10 ppm) as the calibration concentration, recalibrated to 40% (3.41 ppm) based preliminary results. To reduce the likelihood of unexpected early zebrafish death during experimentation, the oxygen regulator was recalibrated before each experiment.

In vivo Imaging and Data Analysis

Larvae to be imaged were transferred to *N*-phenylthiourea to inhibit pigmentation at 24 h post-fertilization (hpf). Prior to imaging, larvae were anesthetized with MS222 and embedded in 1% low-melting-point agarose in embryo medium containing MS222. All images of the spinal cord were taken laterally, such that anterior was to the left, and dorsal was at the top. To investigate OPC migration at 3 and 4 dpf *in vivo*, Tg (*olig2*:EGFP) transgenic zebrafishes were imaged under a 10 × objective lens and a 40 × objective lens (FV1000 BX61; Olympus, Tokyo, Japan) at 2 μm intervals, locating within a frame long and wide with the cloacal pores at the central point of the spinal cord. After imaging, fish were removed from the agarose and placed in fresh embryo medium for further growth. Photomontages were assembled with Adobe Photoshop CS5 (Adobe Systems, San Jose, CA, United States).

Treatment With CoCl₂·6H₂O and LDN193189

Cobalt (II) chloride hexahydrate (CoCl₂·6H₂O; Sangon, China) is a general drug designed to induce hypoxia *in vitro* (Wu et al., 2015). LDN193189 (S2618; Selleck Chemicals, United States) was used as a Bmp2b receptor inhibitor. We treated 1-dpf larvae with either 2 mM CoCl₂·6H₂O or 10 μM LDN193189 in subsequent experiments.

Quantitative Real-Time Polymerase Chain Reaction (qRT-PCR) and Western Blots

Total mRNA was extracted from three groups of 30 larvae each, with each group representing a single independent sample. Each sample was reverse-transcribed into complementary DNA (cDNA) with HiScriptII Q RT SuperMix (Vazyme, China), and analyzed with qRT-PCR using AceQ qPCR SYBR Green Master Mix (Vazyme, China). For each experiment, we used three biological and experimental replicates. All primers used are given in **Supplementary Table S1**. All results were analyzed as mean fold change ± SEM.

To detect protein expression of Mbp, Bmp2b, and Hif1α in zebrafish larvae, we collected normoxic and hypoxic WT zebrafish larvae at 3 and 4 dpf. Larvae were lysed with RIPA buffer (Beyotime, China). Equal amounts of pooled normoxic and hypoxic extracts were loaded onto SDS-PAGE gels. Western blots were performed using the antibodies to Mbp (1:1,000; Abmart, Shanghai, China), Bmp2b (1:1,000; GTX54233; Genetex, Irvine, CA, United States), HIF1α (1:500; NB100-134; Novus), and β-actin (1:1,000; GTX629630;

Genetex, Irvine, CA, United States) as primary antibodies. The MBP rabbit polyclonal antibody was generated (by Abmart, Shanghai, China) using the peptide SRSRSPKRWSTIF as previously described (Lyons et al., 2005). The HRP-conjugated goat anti-rabbit secondary antibody (Invitrogen, Carlsbad, CA, United States) was diluted to 1: 10,000 at room temperature.

Bmp2b mRNA Synthesis and Microinjection

To generate *bmp2b* mRNA, a full-length *bmp2b* fragment was initially amplified from the cDNA of the WT zebrafish strain using a pair of primers (Supplementary Table S1). *bmp2b* mRNA was then synthesized with a T7 mMESSAGE mMACHINE Kit (Ambion, Foster City, CA, United States). Finally, we injected 200 pg *bmp2b* mRNA into single-cell zebrafish embryos.

Zebrafish Optokinetic Response (OKR) Assays

Optokinetic Response assays were performed as previously described (Mueller and Neuhaus, 2010; Huang et al., 2018). We used these assays to visually examine the functional deficiencies of 4-dpf hypoxic zebrafish larvae after OL development disruption. We used LabVIEW to generate a sine-wave grating and used an LCD projector to project this grating. Zebrafish larvae were immobilized dorsal side up in 6% methylcellulose in a chamber. Elicited eye movements were recorded in real time by an infrared-sensitive CCD camera (TCA-1.3BW; Nanjing, China), while rotating grating patterns were projected around the larva. Normoxic and hypoxic larvae were stimulated at a constant angular velocity of 7.5°. To measure visual acuity, both sets of larvae were presented with spatial frequencies of 0.02, 0.04, and 0.06 cycles/degree at 3, 6, and 9 continuous contrast levels, respectively. The OKR gain (the ratio of eye velocity to stimulus velocity) was used to measure contrast sensitivity (Rinner et al., 2005).

Transmission Electron Microscopy

All larval zebrafish were immobilized overnight in a 2.0% formaldehyde and 2.5% glutaraldehyde fixative solution (Electron Microscopy Sciences, United States) at 4°C. Immobilized larval zebrafish were washed with 0.1 M phosphate buffer (pH 7.4). Specimens were then incubated in a postfixation solution containing 1% osmium tetroxide for 2 h and washed with water. Specimens were then washed three times with 0.1 M phosphate buffer (pH 7.4) for 15 min each time. Next, specimens were washed with water, and twice dehydrated with serial dilutions of ethanol in water (i.e., 50, 70, 80, 90, and 100%) and with 100% for 15 min each. All samples were then embedded in epon/araldite resin and hardened for 2 to 3 days at 60°C. Ultrathin (80 nm) transverse sections of the spinal cords of all larvae were stained with uranyl acetate and lead citrate. Sections were viewed and photographed with an FEI Tecnai Spirit (120 kV TEM) transmission electron microscope.

Statistical Analysis

Values were presented as means \pm SEMs. The significance of differences between or among groups were identified using Student's *t*-tests, non-parametric tests, one-way analyses of variance (ANOVA), or two-way ANOVAs, based on the number of groups compared and other independent factors. For qRT-PCR analyses, we analyzed three independent samples three times each to yield reliable results. Statistical significance was classed as follows: **P* < 0.05, ***P* < 0.01, and ****P* < 0.001.

RESULTS

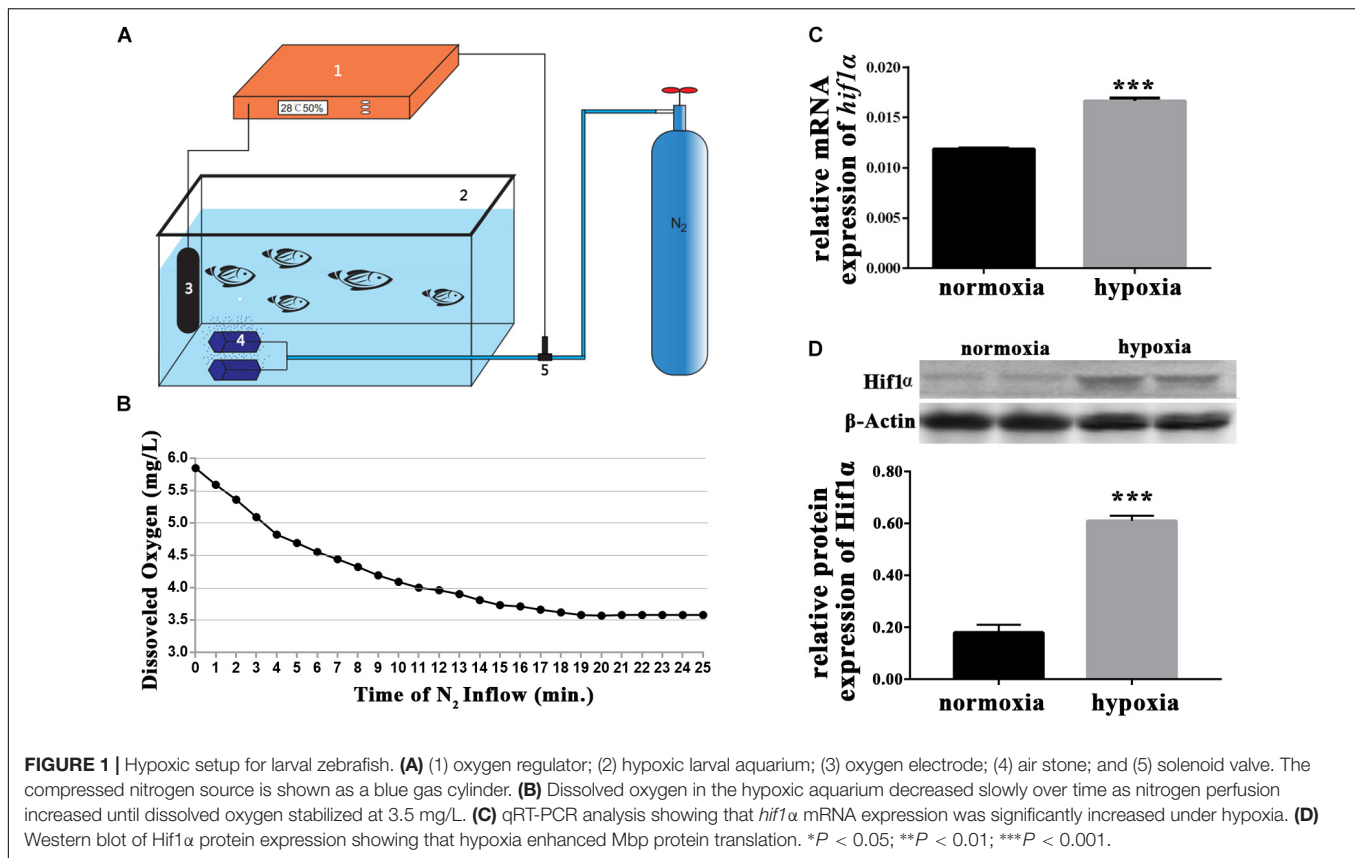
Creation of Moderate Sublethal Hypoxic Conditions for Larval Zebrafish

To create hypoxic conditions for larval zebrafish, nitrogen gas was perfused into the water of a 1 L aquarium. The aquarium was an automated unit (Figure 1A). Oxygen levels were accurately measured by the oxygen electrode, which was connected to the oxygen regulator and the nitrogen gas supplier. Thus, nitrogen gas perfusion was controlled depending on the levels of dissolved oxygen in the water. Preliminary studies indicated that dissolved oxygen levels of 3.5 mg/L were optimal for our experiments (Figure 1B). Preliminary experiments also showed that the gene expression of *hif1 α* and the protein expression of Hif1 α increased in response to hypoxia (Figures 1C,D). Thus, we successfully created sublethal hypoxic conditions by automatically regulating the perfusion of nitrogen into the water.

Hypoxia Suppressed OL Differentiation

In infants with periventricular leukomalacia, the delivery of oxygen to the developing brain often fails; in addition, these infants also exhibit widespread changes in glial maturation, with a loss of myelinated fiber tracts (Haynes et al., 2012). To investigate the OL changes that might occur in the central nervous system *in vivo* in response to hypoxia, we first observed OPC migration in the Tg (*olig2*: EGFP) transgenic line. At 24 hpf, embryos subjected to hypoxia, and larvae were collected for living imaging at 3 and 4 dpf. At both 3 and 4 dpf, significantly fewer dorsally migrated spinal cord *olig2*⁺ cells were observed in the hypoxic larvae (*n* = 10; 3 dpf: 23.30 \pm 1.955; 4 dpf: 25.80 \pm 1.562) (Figure 2B) as compared to the normoxic larvae (*n* = 10; 3 dpf: 44.70 \pm 1.012; 4 dpf: 55.00 \pm 1.921; Figure 2A).

To further test these results, we used cobalt chloride (CoCl₂) to induce similar hypoxia conditions (Goldberg et al., 1988; Wu et al., 2015). At 24 hpf, 2 mM of CoCl₂·6H₂O (Sangon, China) was used to mimic hypoxia. We then collected larvae at 3 and 4 dpf to observe OPC migration. We observed far fewer dorsally migrated spinal cord *olig2*⁺ cells in the CoCl₂·6H₂O group (*n* = 10; 3 dpf: 28.92 \pm 1.803; 4 dpf: 31.69 \pm 1.685) than in the control group (*n* = 10; 3 dpf: 44.70 \pm 1.012; 4 dpf: 55.00 \pm 1.921; Figures 2C,D). This result suggested that some *olig2*⁺ cells differentiated and matured early, beginning functional myelination locally, and were thus unable to migrate to their normal destinations. Together, these results indicated that hypoxia suppresses zebrafish OPC differentiation *in vivo*.



Hypoxia Induced Delayed OL Myelination

To explore the subsequent OL developmental processes, we observed mature OLs. Myelination occurs along an anteroposterior gradient in the developing spinal cord (Buckley et al., 2008). Therefore, we used the timings of the appearance of myelin sheaths at specific sites along the anteroposterior axis as the indices of myelination development. For this experiment, we used Tg (*mbp*:EGFP-CAAX) zebrafish, and found that the onset of myelination was delayed under hypoxia (Figures 3A,B). In normoxic zebrafish larvae, the onset of myelination was 3 dpf, which coincided with *mbp* gene transcription and dorsal OL migration/differentiation (Buckley et al., 2010).

To further evaluate myelination under hypoxia, we used electron microscopy to examine the myelination of zebrafish axons in the spinal cord at 4 dpf (Figures 3C–E and Supplementary Figure S2). We found that many more axons were myelinated than unmyelinated in the normoxic group, whereas the opposite result was observed in the hypoxic and CoCl₂ groups. We then used the G-ratio (the axon circumference divided by the total circumference) to compare the number of myelinated axons between groups (Yin and Hu, 2014). The axon G-ratios in the hypoxic groups ($n = 17$; 0.9144 ± 0.01243) and in the CoCl₂ groups ($n = 11$; 0.9029 ± 0.01559) were also higher than those of the normoxic groups ($n = 17$; 0.8623 ± 0.02167) (Figure 3F).

We further investigated the effects of hypoxia on OPC migration and axonal myelination by quantifying the gene

expression of *mbp* and *olig2* and the protein expression of Mbp in hypoxic zebrafish larvae at 3 dpf and 4 dpf. Our qRT-PCR results showed that at 3, 4, and 5 dpf, *mbp* and *olig2* mRNA expression were significantly lower in hypoxic zebrafish larvae as compared to normoxic larvae (Figure 3G and Supplementary Figure S1). The protein expression of Mbp was also substantially lower in the hypoxia group as compared to the normoxic group (Figure 3H).

Using OKR to assess the function of the visual system, previous studies have also demonstrated that OL affects OKR in zebrafish (Yin and Hu, 2014; Tian et al., 2016). Here, our OKR test revealed that, under hypoxia, central nervous system myelination was delayed and that myelin sheaths were more thinly wrapped. Additionally, our OKR experiment indicated that visual function was also deficient in 4-dpf hypoxic zebrafish (Supplementary Figure S3).

Thus, our results indicated that hypoxia disrupts OL development *in vivo*, both in terms of OPC migration and with respect to mature OL myelination.

LDN193189 Inhibited OPC Dorsal Migration

BMP deficiency affects glial maturation in the spinal cord (See et al., 2007). BMPs also act as growth factors, stimulating axon growth in the spinal motor neurons (Zhong and Zou, 2014). Bmp2b and Bmp4 are two classic BMP isoforms that regulate the early development of zebrafish (Grinspan et al., 2000; Mowbray et al., 2001; Ke et al., 2008; Tiso et al., 2009).

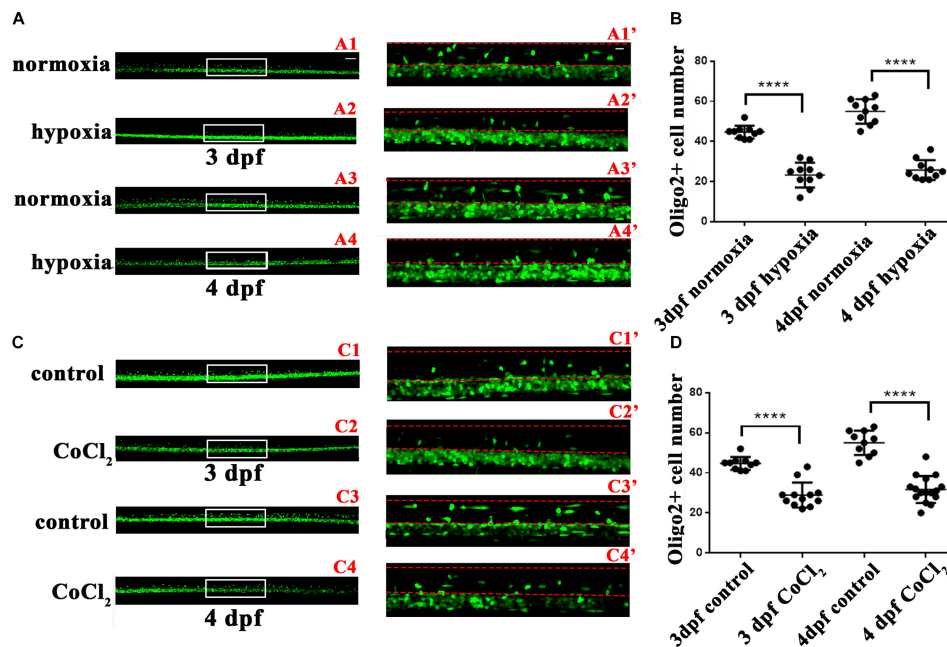


FIGURE 2 | Hypoxia and $\text{CoCl}_2 \cdot 6\text{H}_2\text{O}$ suppressed OPC migration to the dorsal area. The number of dorsally migrated spinal cord *olig2*⁺ cells was counted in Tg (*olig2*: EGFP) zebrafish using a 10 × objective lens on a FV1000 microscope (Olympus, Tokyo, Japan). **(A,B)** The number of dorsally migrated *olig2*⁺ cells decreased under hypoxia at 3 and 4 dpf. A1', A2', A3', and A4' are the magnified pictures of the white boxes in A1, A2, A3, and A4. Two-way ANOVA, $P < 0.0001$: Student's two-tailed *t*-test. Significantly more cells were dorsally migrated in 3-dpf normoxic larvae as compared to 3-dpf hypoxic larvae ($n = 10$; $P < 0.0001$). Significantly more cells were dorsally migrated in 4-dpf normoxic larvae as compared to 4-dpf hypoxic larvae ($n = 10$; $P < 0.0001$). **(C,D)** The number of dorsally migrated spinal cord *olig2*⁺ cells in 3- and 4-dpf larvae decreased after $\text{CoCl}_2 \cdot 6\text{H}_2\text{O}$ exposure. C1', C2', C3', and C4' are the magnified pictures of the white boxes in C1, C2, C3, and C4. Two-way ANOVA, $P < 0.0001$: Student's two-tailed *t*-test. Significantly more cells were dorsally migrated in 3-dpf normoxic larvae as compared to 3-dpf hypoxic larvae ($n = 10$; $P < 0.0001$). Significantly more cells were dorsally migrated in 4-dpf normoxic larvae as compared to 4-dpf hypoxic larvae ($n = 10$; $P < 0.0001$). The dashed line indicates the dorsal spinal cord. Scale bars: A1–A4 and C1–C4, 50 μm ; A1'–A4', and C1'–C4', 10 μm . * $P < 0.05$; ** $P < 0.01$; *** $P < 0.001$. Error bars represent S.E.M.

Therefore, we measured the gene expression of *bmp2b* and *bmp4* with qRT-PCR. We found that *bmp2b* gene expression was strongly downregulated in 3 and 4 dpf hypoxic zebrafish larvae vs. normoxic larvae (Figures 4A,B); there was no apparent change *bmp4* gene expression (data not shown). Bmp2b protein expression was also obviously downregulated in the hypoxic larvae as compared to the normoxic larvae (Figures 4C,D).

We next used a Bmp2b receptor inhibitor to observe OPC migration, and found that significantly fewer spinal cord *olig2*⁺ cells were dorsally migrated in the larvae treated with 10 μM LDN193189 at 3 dpf ($n = 10$; 28.20 ± 2.274) and 4 dpf ($n = 11$; 33.73 ± 1.544), as compared to the untreated larvae at 3 dpf ($n = 10$; 44.70 ± 1.012) and 4 dpf ($n = 10$; 55.00 ± 1.921 ; Figures 4E,F). These results suggested that Bmp2b might play a pivotal role in the regulation of OPC differentiation under hypoxia.

Bmp2b mRNA Reversed the Abnormalities in OPC Differentiation

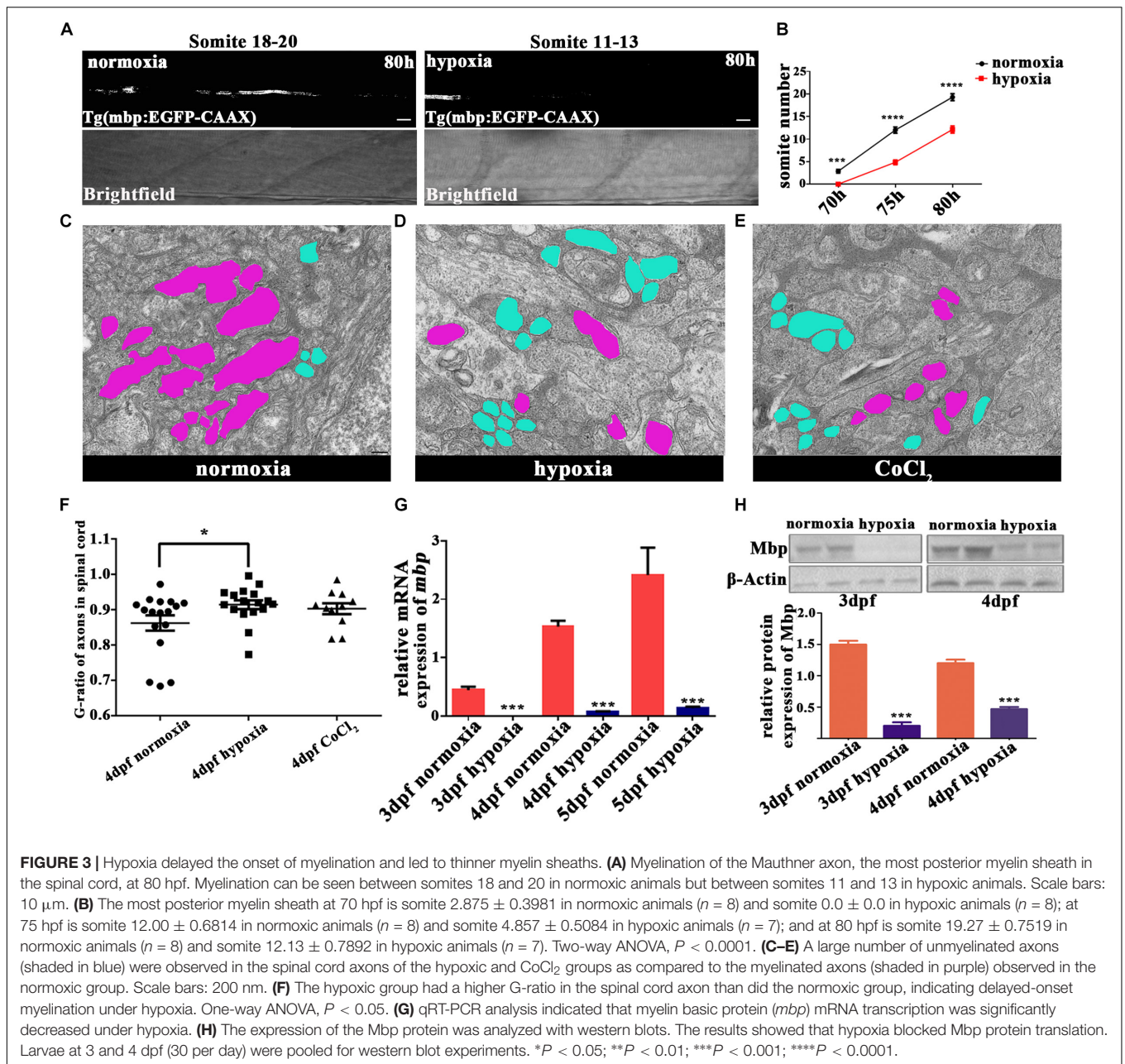
To investigate whether *bmp2b* was essential to OPC migration under hypoxia, we synthesized *bmp2b* mRNA and injected it into one-cell Tg (*olig2*: EGFP) zebrafish embryos. We then measured *bmp2b* gene expression at 3 dpf (Figures 5A,B). We found

that *bmp2b* mRNA injection after CoCl_2 increased the dorsally migrated spinal cord *olig2*⁺ cells at 3 dpf ($n = 15$; 35.53 ± 1.521) and 4 dpf ($n = 17$; 31.06 ± 1.459), as compared to CoCl_2 -treated larvae not injected with *bmp2b* mRNA at 3 dpf ($n = 12$; 28.92 ± 1.803) and 4 dpf ($n = 16$; 31.69 ± 1.685 ; Figures 5C,D). These results indicated that Bmp2b signaling is critical to OPC differentiation.

DISCUSSION

Hypoxia is a principal cause of brain injury in premature infants, which clinical features consist of diagnostic aspects and clinicopathologic correlations (du Plessis, 2009). Using a hypoxic larval zebrafish model, we identified several novel aspects of OL behavior in the spinal cord under hypoxia. First, we used Tg (*olig2*: EGFP) and Tg (*mbp*-EGFP-CAAX) hypoxic models to show that fewer OPCs migrated to the dorsal area and that myelin sheaths in the spinal cord were thinner. Second, *bmp2b* gene expression was downregulated in hypoxic animals. Third, based on loss of function and gain of function, we demonstrated that hypoxia suppressed OL differentiation through Bmp2b signaling.

Hypoxia affects many processes involved in bone regeneration (Drager et al., 2015) and angiogenesis



(Tanaka and Nangaku, 2013). Several rodent models have been designed to study various hypoxia-induced diseases, including retinopathy (Liu et al., 2014), bronchopulmonary dysplasia (Elberson et al., 2015), and absolutely periventricular leukomalacia (Chen et al., 2015). However, the zebrafish has become an attractive vertebrate model organism for the study of hypoxia-induced diseases due to the broad conservation of its genes and its bodily transparency (Cao et al., 2010; Wu et al., 2015). Here, we observed OPC migration and OL myelination *in vivo*. We found that, under hypoxia, significantly fewer *olig2*⁺ cells migrated to the dorsal area, and *olig2* gene expression was downregulated. The onset of myelination was also delayed under hypoxia, which may have been due to changes in *mbp*

transcription and dorsal OL migration and differentiation (Buckley et al., 2010). We used TEM to show that spinal cord axons were covered with a thinner myelin sheath under hypoxia, indicating that hypoxia severely disrupted OL function. Our results thus indicated that hypoxia affected OPC migration, OL myelination, and even myelin sheath thickness.

We also investigated the effects of Bmp2b on OL differentiation under hypoxia using loss of function and gain of function. Consistent with our results, BMPs have been shown to be associated with OPC differentiation (See et al., 2007). Although the mechanisms by which hypoxia affects Bmp2b expression, several studies have shown that BMPs are associated with OL differentiation, and that hypoxia affects BMP2

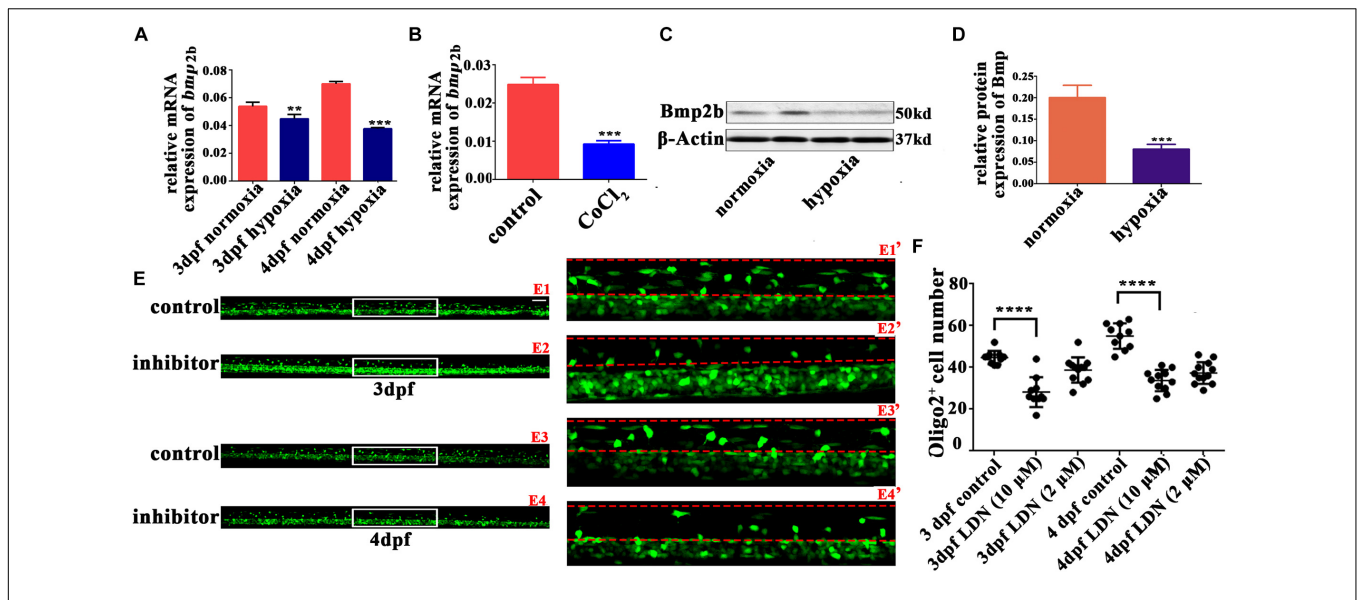


FIGURE 4 | The *Bmp2b* inhibitor suppresses OPC migration to the dorsal area. **(A,B)** qRT-PCR analysis indicated that *bmp2b* gene mRNA expression was significantly downregulated after hypoxia and CoCl_2 exposure. **(C,D)** *Bmp2b* protein expression was analyzed with western blots. The results showed that hypoxia blocked *Bmp2b* protein translation. Thirty zebrafish 4-dpf larvae were pooled for western blots experiments. **(E,F)** The number of dorsally migrated *olig2*⁺ cells at 3 and 4 dpf decreased after LDN193189 treatment. E1', E2', E3', and E4' are magnified pictures of the white boxes in E1, E2, E3, and E4. Scale bars: E1–E4, 50 μm and E1'–E4', 10 μm . Two-way ANOVA, $P < 0.0001$; Student's two-tailed *t*-test. Significantly more cells were dorsally migrated in 3-dpf control larvae as compared to 3-dpf larvae treated with 10 μM LDN193189 ($n = 12$; $P < 0.0001$). Significantly more cells were dorsally migrated in 4-dpf normoxic larvae as compared to 4-dpf larvae treated with 10 μM LDN193189 ($n = 10$; $P < 0.0001$). * $P < 0.05$; ** $P < 0.01$; *** $P < 0.001$; **** $P < 0.0001$. Error bars represent S.E.M.

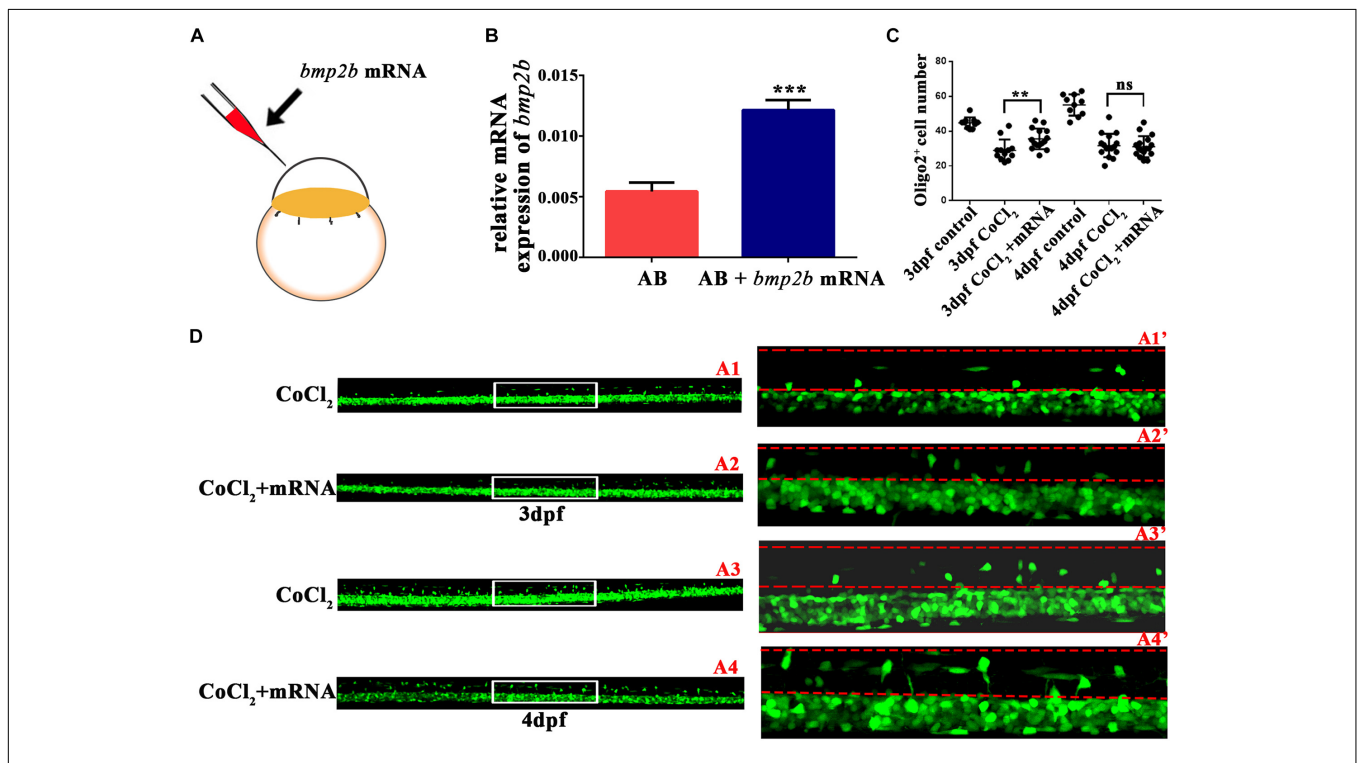


FIGURE 5 | *Bmp2b* mRNA reversed the reduction in the number of *olig2*⁺ cells migrating to the dorsal area. **(A)** *Bmp2b* mRNA was injected into one-cell embryos. **(B)** qRT-PCR analysis showed that *bmp2b* gene expression increased, validating the rescue effect. **(C–D)** *bmp2b* mRNA reversed the reduction in the number of dorsally migrated *olig2*⁺ cells at 3 and 4 dpf. A1', A2', A3', and A4' are the magnified pictures of the white boxes in A1, A2, A3, and A4. Scale bars: A1–A4, 50 μm and A1'–A4', 10 μm . * $P < 0.05$; ** $P < 0.01$; *** $P < 0.001$. Error bars represent S.E.M.

protein expression (Drager et al., 2015). Thus, we speculated that *Bmp2b* might be involved in reducing OL differentiation in zebrafish. However, our results do not exclude the possibility that additional genes or BMP subunits may also be regulated by hypoxia.

To test our speculation, we designed *bmp2b* rescue mRNA. For the OPC migration experiment, we obtained the desired rescue effect by injecting *bmp2b* mRNA into one-cell-phase embryos.

CONCLUSION

In summary, our results indicated that hypoxia negatively influences OL differentiation, and that this process was mediated by *Bmp2b* signaling. Our ultimately increases our understanding of hypoxia and glial development.

AUTHOR CONTRIBUTIONS

L-qY, D-IR, and BH designed the experiments. L-qY conducted all the experiments and wrote the manuscript. MC and J-IZ also

helped to complete part of the experiments. BH and D-IR revised the manuscript.

FUNDING

This research was supported by grants from National Natural Science Foundation of China (81790643, 31701027, and 31771183), Anhui Provincial Natural Science Foundation (1708085QC58).

ACKNOWLEDGMENTS

We thank our Core Facility Center for Life Sciences, University of Science and Technology of China.

SUPPLEMENTARY MATERIAL

The Supplementary Material for this article can be found online at: <https://www.frontiersin.org/articles/10.3389/fncel.2018.00348/full#supplementary-material>

REFERENCES

- Accorsi-Mendonca, D., Almado, C. E., Bonagamba, L. G., Castania, J. A., Moraes, D. J., and Machado, B. H. (2015). Enhanced firing in NTS induced by short-term sustained hypoxia is modulated by Glia-Neuron interaction. *J. Neurosci.* 35, 6903–6917. doi: 10.1523/JNEUROSCI.4598-14.2015
- Almeida, R. G., Czopka, T., Ffrench-Constant, C., and Lyons, D. A. (2011). Individual axons regulate the myelinating potential of single oligodendrocytes in vivo. *Development* 138, 4443–4450. doi: 10.1242/dev.071001
- Back, S. A., Craig, A., Luo, N. L., Ren, J., Akundi, R. S., Ribeiro, I., et al. (2006). Protective effects of caffeine on chronic hypoxia-induced perinatal white matter injury. *Ann. Neurol.* 60, 696–705. doi: 10.1002/ana.21008
- Buckley, C. E., Goldsmith, P., and Franklin, R. J. (2008). Zebrafish myelination: a transparent model for remyelination? *Dis. Model. Mech.* 1, 221–228. doi: 10.1242/dmm.001248
- Buckley, C. E., Marguerie, A., Alderton, W. K., and Franklin, R. J. (2010). Temporal dynamics of myelination in the zebrafish spinal cord. *Glia* 58, 802–812. doi: 10.1002/glia.20964
- Cao, Z., Jensen, L. D., Rouhi, P., Hosaka, K., Lanne, T., Steffensen, J. F., et al. (2010). Hypoxia-induced retinopathy model in adult zebrafish. *Nat. Protoc.* 5, 1903–1910. doi: 10.1038/nprot.2010.149
- Chahboune, H., Ment, L. R., Stewart, W. B., Rothman, D. L., Vaccarino, F. M., Hyder, F., et al. (2009). Hypoxic injury during neonatal development in murine brain: correlation between in vivo DTI findings and behavioral assessment. *Cereb. Cortex* 19, 2891–2901. doi: 10.1093/cercor/bhp068
- Chen, L. X., Ma, S. M., Zhang, P., Fan, Z. C., Xiong, M., Cheng, G. Q., et al. (2015). Neuroprotective effects of oligodendrocyte progenitor cell transplantation in premature rat brain following hypoxic-ischemic injury. *PLoS One* 10:e0115997. doi: 10.1371/journal.pone.0115997
- Currustin, S. M., Cao, A., Stewart, W. B., Zhang, H., Madri, J. A., Morrow, J. S., et al. (2002). Disrupted synaptic development in the hypoxic newborn brain. *Proc. Natl. Acad. Sci. U.S.A.* 99, 15729–15734. doi: 10.1073/pnas.232568799
- Drager, J., Harvey, E. J., and Barralet, J. (2015). Hypoxia signalling manipulation for bone regeneration. *Expert Rev. Mol. Med.* 17:e6. doi: 10.1017/erm.2015.4
- du Plessis, A. J. (2009). Neurology of the newborn infant. Preface. *Clin. Perinatol.* 36, 11–13.
- Dubois-Dalcq, M., Williams, A., Stadelmann, C., Stankoff, B., Zalc, B., and Lubetzki, C. (2008). From fish to man: understanding endogenous remyelination in central nervous system demyelinating diseases. *Brain* 131, 1686–1700. doi: 10.1093/brain/awn076
- Elberson, V. D., Nielsen, L. C., Wang, H., and Kumar, H. S. (2015). Effects of intermittent hypoxia and hyperoxia on angiogenesis and lung development in newborn mice. *J. Neonatal Perinatal Med.* 8, 313–322. doi: 10.3233/NPM-15814134
- Fagel, D. M., Ganat, Y., Cheng, E., Silbereis, J., Ohkubo, Y., Ment, L. R., et al. (2009). *Fgfr1* is required for cortical regeneration and repair after perinatal hypoxia. *J. Neurosci.* 29, 1202–1211. doi: 10.1523/JNEUROSCI.4516-08.2009
- Ganat, Y., Soni, S., Chacon, M., Schwartz, M. L., and Vaccarino, F. M. (2002). Chronic hypoxia up-regulates fibroblast growth factor ligands in the perinatal brain and induces fibroblast growth factor-responsive radial glial cells in the sub-ependymal zone. *Neuroscience* 112, 977–991. doi: 10.1016/S0306-4522(02)00060-X
- Goldberg, M. A., Dunning, S. P., and Bunn, H. F. (1988). Regulation of the erythropoietin gene: evidence that the oxygen sensor is a heme protein. *Science* 242, 1412–1415. doi: 10.1126/science.2849206
- Grinspan, J. B., Edell, E., Carpio, D. F., Beesley, J. S., Lavy, L., Pleasure, D., et al. (2000). Stage-specific effects of bone morphogenetic proteins on the oligodendrocyte lineage. *J. Neurobiol.* 43, 1–17. doi: 10.1002/(SICI)1097-4695(200004)43:1<1::AID-NEU1>3.0.CO;2-0
- Hack, M., Taylor, H. G., Klein, N., and Mercuri-Minich, N. (2000). Functional limitations and special health care needs of 10- to 14-year-old children weighing less than 750 grams at birth. *Pediatrics* 106, 554–560. doi: 10.1542/peds.106.3.554
- Haynes, R. L., Desilva, T. M., and Li, J. (2012). Mechanisms of perinatal brain injury. *Neurol. Res. Int.* 2012:157858. doi: 10.1155/2012/157858
- He, J. H., Gao, J. M., Huang, C. J., and Li, C. Q. (2014). Zebrafish models for assessing developmental and reproductive toxicity. *Neurotoxicol. Teratol.* 42, 35–42. doi: 10.1016/j.ntt.2014.01.006
- Huang, D. F., Wang, M. Y., Yin, W., Ma, Y. Q., Wang, H., Xue, T., et al. (2018). Zebrafish lacking circadian gene *per2* exhibit visual function deficiency. *Front. Behav. Neurosci.* 12:53. doi: 10.3389/fnbeh.2018.00053
- Huppi, P. S., Murphy, B., Maier, S. E., Zientara, G. P., Inder, T. E., Barnes, P. D., et al. (2001). Microstructural brain development after perinatal cerebral white matter injury assessed by diffusion tensor magnetic resonance imaging. *Pediatrics* 107, 455–460. doi: 10.1542/peds.107.3.455
- Kanaan, A., Farahani, R., Douglas, R. M., Lamanna, J. C., and Haddad, G. G. (2006). Effect of chronic continuous or intermittent hypoxia and reoxygenation on

- cerebral capillary density and myelination. *Am. J. Physiol. Regul. Integr. Comp. Physiol.* 290, R1105–R1114. doi: 10.1152/ajpregu.00535.2005
- Ke, Z., Kondrichin, I., Gong, Z., and Korzh, V. (2008). Combined activity of the two Gli2 genes of zebrafish play a major role in Hedgehog signaling during zebrafish neurodevelopment. *Mol. Cell. Neurosci.* 37, 388–401. doi: 10.1016/j.mcn.2007.10.013
- Kimmel, C. B., Ballard, W. W., Kimmel, S. R., Ullmann, B., and Schilling, T. F. (1995). Stages of embryonic development of the zebrafish. *Dev. Dyn.* 203, 253–310. doi: 10.1002/aja.1002030302
- Kumar, V., and Gabrilovich, D. I. (2014). Hypoxia-inducible factors in regulation of immune responses in tumour microenvironment. *Immunology* 143, 512–519. doi: 10.1111/imm.12380
- Liu, N., Sun, Y., Zhao, N., and Chen, L. (2014). Role of hypoxia-inducible factor-1alpha and survivin in oxygen-induced retinopathy in mice. *Int. J. Clin. Exp. Pathol.* 7, 6814–6819.
- Lyons, D. A., Pogoda, H. M., Voas, M. G., Woods, I. G., Diamond, B., Nix, R., et al. (2005). *erbb3* and *erbb2* are essential for schwann cell migration and myelination in zebrafish. *Curr. Biol.* 15, 513–524. doi: 10.1016/j.cub.2005.02.030
- Maes, C., Carmeliet, G., and Schipani, E. (2012). Hypoxia-driven pathways in bone development, regeneration and disease. *Nat. Rev. Rheumatol.* 8, 358–366. doi: 10.1038/nrrheum.2012.36
- Mowbray, C., Hammerschmidt, M., and Whitfield, T. T. (2001). Expression of BMP signalling pathway members in the developing zebrafish inner ear and lateral line. *Mech. Dev.* 108, 179–184. doi: 10.1016/S0925-4773(01)00479-8
- Mueller, K. P., and Neuhauss, S. C. (2010). Quantitative measurements of the optokinetic response in adult fish. *J. Neurosci. Methods* 186, 29–34. doi: 10.1016/j.jneumeth.2009.10.020
- Paltsyn, A. A., Manukhina, E. B., Goryacheva, A. V., Downey, H. F., Dubrovin, I. P., Komissarova, S. V., et al. (2014). Intermittent hypoxia stimulates formation of binuclear neurons in brain cortex- a role of cell fusion in neuroprotection? *Exp. Biol. Med.* 239, 595–600. doi: 10.1177/1535370214523898
- Rinner, O., Rick, J. M., and Neuhauss, S. C. (2005). Contrast sensitivity, spatial and temporal tuning of the larval zebrafish optokinetic response. *Invest. Ophthalmol. Vis. Sci.* 46, 137–142. doi: 10.1167/iovs.04-0682
- Sabatino, G. M., Domizio, S., Cicioni, P., and Sabatino, G. (2003). Mechanisms of perinatal brain injury. *Panminerva Med.* 45, 117–121.
- Satou, C., Kimura, Y., Kohashi, T., Horikawa, K., Takeda, H., Oda, Y., et al. (2009). Functional role of a specialized class of spinal commissural inhibitory neurons during fast escapes in zebrafish. *J. Neurosci.* 29, 6780–6793. doi: 10.1523/JNEUROSCI.0801-09.2009
- Scafidi, J., Hammond, T. R., Scafidi, S., Ritter, J., Jablonska, B., Roncal, M., et al. (2014). Intranasal epidermal growth factor treatment rescues neonatal brain injury. *Nature* 506, 230–234. doi: 10.1038/nature12880
- See, J., Mamontov, P., Ahn, K., Wine-Lee, L., Crenshaw, E. B. III, and Grinspan, J. B. (2007). BMP signaling mutant mice exhibit glial cell maturation defects. *Mol. Cell. Neurosci.* 35, 171–182. doi: 10.1016/j.mcn.2007.02.012
- Shin, J., Park, H. C., Topczewska, J. M., Mawdsley, D. J., and Appel, B. (2003). Neural cell fate analysis in zebrafish using olig2 BAC transgenics. *Methods Cell Sci.* 25, 7–14. doi: 10.1023/B:MICS.0000006847.09037.3a
- Tanaka, T., and Nangaku, M. (2013). Angiogenesis and hypoxia in the kidney. *Nat. Rev. Nephrol.* 9, 211–222. doi: 10.1038/nrneph.2013.35
- Tian, C., Zou, S., and Hu, B. (2016). Extraocular source of oligodendrocytes contribute to retinal myelination and optokinetic responses in zebrafish. *Invest. Ophthalmol. Vis. Sci.* 57, 2129–2138. doi: 10.1167/iovs.15-17675
- Tiso, N., Filippi, A., Benato, F., Negrisolo, E., Modena, N., Vaccari, E., et al. (2009). Differential expression and regulation of olig genes in zebrafish. *J. Comp. Neurol.* 515, 378–396. doi: 10.1002/cne.22054
- Watzlawik, J. O., Kahoud, R. J., O'Toole, R. J., White, K. A., Ogden, A. R., Painter, M. M., et al. (2015). Abbreviated exposure to hypoxia is sufficient to induce CNS dysmyelination, modulate spinal motor neuron composition, and impair motor development in neonatal mice. *PLoS One* 10:e0128007. doi: 10.1371/journal.pone.0128007
- Weiss, J., Takizawa, B., McGee, A., Stewart, W. B., Zhang, H., Ment, L., et al. (2004). Neonatal hypoxia suppresses oligodendrocyte Nogo-A and increases axonal sprouting in a rodent model for human prematurity. *Exp. Neurol.* 189, 141–149. doi: 10.1016/j.expneurol.2004.05.018
- Wu, Y. C., Chang, C. Y., Kao, A., Hsi, B., Lee, S. H., Chen, Y. H., et al. (2015). Hypoxia-induced retinal neovascularization in zebrafish embryos: a potential model of retinopathy of prematurity. *PLoS One* 10:e0126750. doi: 10.1371/journal.pone.0126750
- Yin, W., and Hu, B. (2014). Knockdown of Lingo1b protein promotes myelination and oligodendrocyte differentiation in zebrafish. *Exp. Neurol.* 251, 72–83. doi: 10.1016/j.expneurol.2013.11.012
- Zhong, J., and Zou, H. (2014). BMP signaling in axon regeneration. *Curr. Opin. Neurobiol.* 27, 127–134. doi: 10.1016/j.conb.2014.03.009
- Zhou, D., Wang, J., Zapala, M. A., Xue, J., Schork, N. J., and Haddad, G. G. (2008). Gene expression in mouse brain following chronic hypoxia: role of sarcospan in glial cell death. *Physiol. Genomics* 32, 370–379. doi: 10.1152/physiolgenomics.00147.2007

Conflict of Interest Statement: The authors declare that the research was conducted in the absence of any commercial or financial relationships that could be construed as a potential conflict of interest.

Copyright © 2018 Yang, Chen, Zhang, Ren and Hu. This is an open-access article distributed under the terms of the Creative Commons Attribution License (CC BY). The use, distribution or reproduction in other forums is permitted, provided the original author(s) and the copyright owner(s) are credited and that the original publication in this journal is cited, in accordance with accepted academic practice. No use, distribution or reproduction is permitted which does not comply with these terms.